Local structure order assisted two-step crystal nucleation in polyethylene

Xiaoliang Tang,[1] Junsheng Yang,[1,2] Tingyu Xu,[1] Fucheng Tian,[1] Chun Xie,[1] and Liangbin Li[1,*]

[1]*National Synchrotron Radiation Lab and CAS Key Laboratory of Soft Matter Chemistry, Anhui Provincial Engineering Laboratory of Advanced Functional Polymer Film, University of Science and Technology of China, Hefei 230026, China*

[2]*Computational Physics Key Laboratory of Sichuan Province, Yibin University, Yibin 644000, China*

(Received 19 January 2017; published 8 December 2017)

The homogeneous nucleation process of polyethylene (PE) is studied with full-atom molecular dynamic simulation. To account for the complex shape with low symmetry and the peculiar intrachain conformational order of polymer, we introduce a shape descriptor O_{CB} coupling conformational order and interchain rotational symmetry, which is able to differentiate hexagonal and orthorhombic clusters from melt. With the shape descriptor O_{CB}, we find that coupling between conformational and interchain rotational orderings results in the formation of hexagonal clusters first, which is dynamic in nature. After the formation of hexagonal clusters, the nucleation of orthorhombic structure occurs inside of them, which proceeds via the coalescence of neighboring hexagonal clusters rather than a standard stepwise growth process. This demonstrates that nucleation of PE crystal is an O_{CB} order assisted two-step process, which is different from previous models for polymer crystallization but similar with that proposed for spherical "atoms" such as colloid and metal.

DOI: 10.1103/PhysRevMaterials.1.073401

I. INTRODUCTION

Crystal nucleation from supercooled liquids is a fundamental phase transition [1] phenomenon universal to materials as well as biological systems. With density as the single order parameter, classical nucleation theory (CNT) [2] and density functional theories (DFT) [3] provide a framework of one-step liquid-solid transition to depict nucleation successfully on a qualitative level, while it is hard to test their predictions such as on nucleation rate at different conditions quantitatively [4–8], and the molecular details of nucleation still remain elusive. Approaching the molecular mechanism of nucleation by the two-step nucleation models, involving either density [5,9,10] or bond-orientational order fluctuation [6,11–13] prior to crystallization, have been proposed. Although their molecular pathways are not the same, both scenarios emphasize the importance of precursor on nucleation. The existence of precursor during nucleation has been widely reported by computer simulations and experiments on spherical "atoms" such as colloid and metal [6,14–17], as well as complex molecules like protein and synthetic polymers [5,18–21], suggesting that a two-step nucleation process may indeed be a general mechanism of nucleation. Nevertheless, current discussion on bond-orientational order assisted nucleation is mainly restricted in spherical atom systems such as colloid and metal with high symmetry, which is rarely mentioned in the nucleation of complex molecular systems like polymer [19,22,23]. For particles with arbitrary shapes or polymers with complex structures, a local structure order may be defined by a shape descriptor with a specific mathematic fingerprint.

Two-step or multistep nucleation scenarios with conformational order or density fluctuation [24–28] have also been proposed to challenge the standard Hoffman-Lauritzen (HL) polymer crystallization model [29]. Crystallization of synthetic and natural polymers shares the common nucleation mechanism of small molecules and yet has its own peculiar features, which are related to industrial processing of about 2 billion tons of semicrystalline polymeric materials annually as well as protein diseases like Alzheimer's and Parkinson's. Due to connectivity and flexibility of long chains, polymer crystallization involves not only orderings like interchain position or orientation, but also intrachain conformational ordering like *gauche-trans* or coil-helix transitions, which introduces a new ordering dimension as compared with spherical "atoms" and small molecules. Although conformational ordering is the most peculiar and critical step in polymer crystallization, the transformation of flexible chains into conformational ordered rigid segments remains nearly untouched. If two-step crystal nucleation is applicable for all materials, local structure order or density fluctuation should also occur in polymer crystallization. Considering the peculiar zigzag or helical conformation in polymer crystal, the shape descriptor defining local structure order should incorporate intrachain conformational order and rotational symmetries of all neighboring atoms (atoms from the same and different chain segments).

In this work, crystal nucleation of polyethyle (PE) with full-atom molecular dynamic computer simulation is studied. In order to define the local structure order of PE, we introduce a shape descriptor or order parameter (defined as O_{CB}) coupling conformational order and interchain order, while the reliability of O_{CB} on extracting ordered structure is verified by structure entropy S_2 as thermodynamic indicator. Density order parameter is expressed by Voronoi volume V. With hexagonal and orthorhombic symmetries of PE crystal as shape matching targets, we define their corresponding O_{CB} and named as H-O_{CB} and O-O_{CB} respectively. We note that only positions of carbon atoms are considered in this work including parameter definition and calculation. The simulation details and the definitions of parameters are presented in section Methods. By analyzing the simulation results with the shape descriptor O_{CB} and Voronoi volume V, we show that two-step nucleation process indeed occurs in PE. At isothermal-isobaric condition, local structures defined as H-O_{CB} with symmetry matches with hexagonal crystal form stochastically first,

*Correspondence author: lbli@ustc.edu.cn

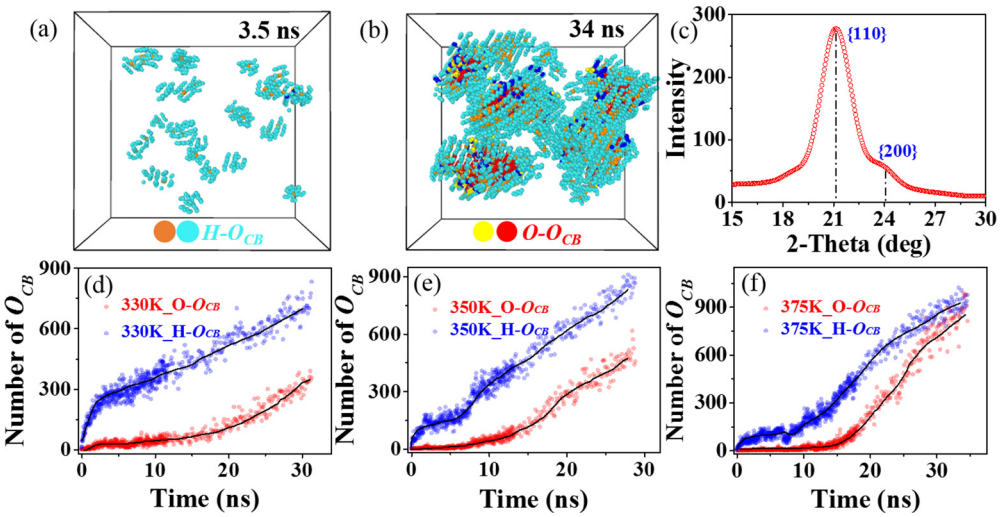

FIG. 1. (a, b) Snapshots of the nucleation process of PE with different types of atoms colored differently. Orange and cyan (red and yellow) correspond the center atom and neighboring atoms of H-O_{CB} (O-O_{CB}) clusters, respectively, while the blue ones belong to both. (c) The XRD of the orthorhombic clusters. (d, e, f) The evolutions of the number of O_{CB} structures at 330, 350, and 375 K, respectively.

followed by emergence of the stable orthorhombic nuclei inside the hexagonal clusters, during which local structure order fluctuation is of significant importance in assisting nucleation.

II. RESULTS

A. Nucleation process of PE

Snapshots of nucleation process of PE at two representative times and 375 K are shown in Figs. 1(a) and 1(b), respectively (only O_{CB} structures are displayed). As indicated in Fig. 1(a), small clusters with O_{CB} value (cyan) matching hexagonal symmetry (H-O_{CB}) form stochastically. These hexagonal clusters appear and disappear dynamically; however, they grow in size with elapsed time. When the hexagonal clusters reach a critical size, an orthorhombic structure emerges inside the hexagonal clusters. Figure 1(b) shows that the orthorhombic structures O-O_{CB} (red) are embedded inside the O_{CB} atoms of hexagonal clusters (cyan). These orthorhombic structures are stable and grow continuously with time. Figure 1(c) shows the x-ray diffraction (XRD) data for orthorhombic domain embedded in the H-O_{CB} structures at 34 ns and 375 K; the peaks at $2\theta = 21.2^\circ$ and 24.2° correspond to the $\{110\}$ and $\{200\}$ crystal planes, respectively. Due to the short lifetime and small size, the hexagonal clusters found in this work are not regarded as hexagonal phase as that at elevated pressures. Indeed, these H-O_{CB} clusters possess only conformational and interchain rotational orders, while no orientational order is required [see Supplemental Material (SM), movie 1] [30] and their density is comparable to the density of melt, as will be shown later. Thus crystal nucleation of PE is demonstrated as a two-step process assisted by the coupling between conformational and interchain rotational orders, which is further confirmed by simulations at 330 and 350 K.

The evolution of the number of O_{CB} structures is calculated (counted by the number of center atoms) and represents the nucleation kinetics, which are depicted in Figs. 1(d)–1(f) for 330, 350, and 375 K, respectively. At all three temperatures, hexagonal clusters (blue) emerge immediately after quenching, while nucleation of the orthorhombic structure (red) always requires incubation times which are about 3.6, 7.5, and 14.0 ns at 330, 350, and 375 K, respectively. The temperature dependence of incubation time indicates that higher supercooling favors the nucleation. On the contrary, higher supercooling corresponds to slower growth rate, as shown in Figs. 1(d) and 1(f). The temperature dependence of nucleation and growth rates observed in the simulations corresponds well with experimental observations as well as the prediction of CNT.

B. H-O_{CB} order independent from density

Formation of H-O_{CB} clusters have reduced structure entropy (S_2), which can provide a practical measure of disorder in the system and prove the reliability of the O_{CB} order parameter. For completely disordered systems S_2 equals 0 (i.e., the ideal gas), which becomes negative for ordered structures ($S_2 \to -\infty$ for perfect crystal) [31]. In order to follow the evolution of S_2 during the formation and the vanishing process of the H-O_{CB} clusters, O_{CB}s at a specific time before 7.5 ns are selected and S_2 of these atoms at time range of 200 ps with step of 5 ps are calculated as Eq. (1), where $g(r)$ is the radial distribution of carbon atoms and ρ the local density within r_c (20 Å in this work). Figure 2(a) presents the evolution of S_2 of H-O_{CB} clusters at five selected times at 375 K, in which the black dash line indicates the formation time of H-O_{CB} clusters. Prior to the formation time, a decline of S_2 can be noticed during the formation of H-O_{CB} clusters, resulting in a local minimum of S_2 [blue region in Fig. 2(a)]. Over 20 representatives were calculated and the tendency remains the same, confirming that the shape descriptor O_{CB} parameter indeed represents ordered structure with low structure entropy.

To clarify whether O_{CB} order couples with density, the Voronoi volume of O_{CB} clusters at different stages is calculated. O_{CB} structures (right column) in a subcube at 375 K

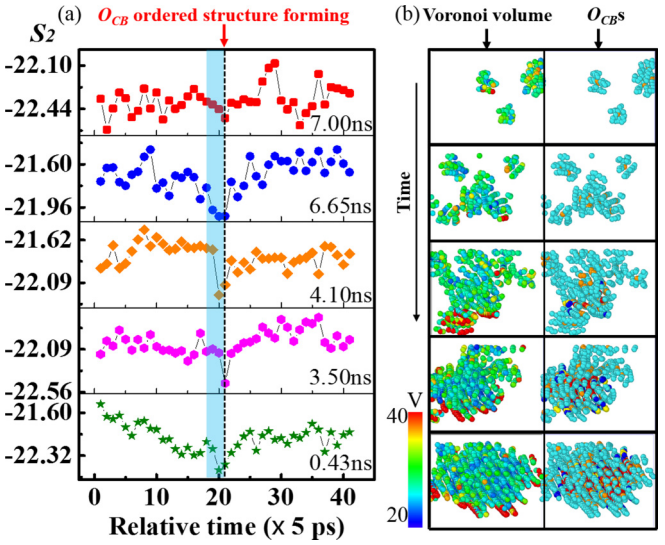

FIG. 2. (a) The S_2 evolution of H-O_{CB} at five representative times before 7.5 ns. The black dashed line indicates the formation time of H-O_{CB} clusters, at which S_2 shows a local minimum. (b) O_{CB} structures (right column) and their Voronoi volume of carbon atoms (left column) at five representative times, where high Voronoi volume means low density. There seems to be no direct correlation between H-O_{CB} and density observed.

and their Voronoi volume of carbon atoms (left column) are shown in Fig. 2(b). O_{CB} structures are colored the same with Fig. 1, and the color-bar for Voronoi volume is at the bottom left corner. The emergence of H-O_{CB} clusters is not accompanied with the change of density as the significant part of Voronoi volume remains constant (green color indicates Voronoi volume ≈30). Densification can only be distinguished after the formation of orthorhombic cores as the Voronoi volume shifts to lower value (blue indicates Voronoi value <25) at orthorhombic regions. Note that the density of H-O_{CB} clusters is relatively low even at the end of simulation. In SM Fig. S2 [30], a direct comparing of density between H-O_{CB} clusters and melt also indicates there is no direct correlation between H-O_{CB} and density. Evidently, H-O_{CB} and density are two independent orderings which are not coupled with each other, while the formation of orthorhombic structure involves the coupling of density and O_{CB} orders. Combining the results from Figs. 2(a) and 2(b), the reduction of S_2 can be attributed to O_{CB} order rather than density, as the latter keeps nearly constant in this stage:

$$S_2 = -\frac{\rho}{2}\int_0^{r_c} dr\{g(r)\times lng(r) - [g(r)-1]\}. \qquad (1)$$

C. Coupling of orders and two-step nucleation

The issue of how the O_{CB} and density couple with each other to form stable orthorhombic nuclei remains unanswered. Figure 3(a) depicts the evolution of the number of clusters and the size of the largest cluster in a sub-box over the time at 375 K, in which a grain crystal at 34 ns is contained. Adjacent-averaged data was shown in SM Fig. S3 [30] to be intuitive observed. The clusters are counted as follows: two clusters are counted as two if their nearest distance is larger than a threshold

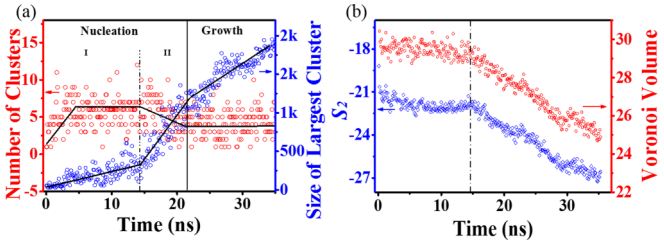

FIG. 3. (a) The evolutions of the number of ordered clusters and the size of the largest cluster in a representative region of the system at 375 K. Nucleation of PE is defined by two steps, namely, O_{CB} fluctuation (step I) and orthorhombic nucleation (step II). (b) The evolutions of structural entropy S_2 and Voronoi volume of carbon atoms at 375 K.

value (5.4 Å in this work), otherwise, they are regarded as a single cluster and counted as one. The size is represented by the number of carbon atoms in one cluster. The evolution of number and size of cluster can be divided into two-step nucleation and one growth stage. In step I of nucleation (0–14.0 ns), the number of clusters (red with black guide line) first increases and fluctuates around 6, and meanwhile the cluster (blue with black guide line) grows slowly. Step I is defined as H-O_{CB} fluctuation because only hexagonal clusters form. The orthorhombic nuclei emerge in step II (14.0–21.0 ns), which is defined as an orthorhombic nucleation step with coupling between O-O_{CB} and density. In step II, a rapid growth of cluster is accompanied with a sharp decrease of the cluster number, suggesting that the formation of orthorhombic nuclei proceeds via a coalescence of neighboring H-O_{CB} clusters. A movie of the simulation process is presented in the SM to confirm the coalescence mechanism [30] (see SM, movie 2). Intuitively, merging neighboring H-O_{CB} clusters seems kinetically more favorable than following the stepwise growth process suggested by CNT [2]. After the formation of stable orthorhombic nuclei at 20 ns, the number of clusters remains small and the size of the cluster continuously increases, which is the growth stage illustrated in Fig. 3(a).

Accompanied by the formation of orthorhombic nuclei, sharp transitions on density and S_2 are also observed. We calculate averaged S_2 and the Voronoi volume of the atoms belong to O-O_{CB} structures, as these atoms experienced the two-step nucleation and the growth processes, which are plotted as a function of time in Fig. 3(b). In step I of nucleation, the Voronoi volume keeps relatively constant while S_2 shows a slight decrease. Once the system enters step II, these two parameters immediately decrease. The evolution of Voronoi volume supports that H-O_{CB} is independent of density in step I, while the formation of orthorhombic nuclei in step II does involve coupling between O_{CB} and density.

The two-step nucleation process is also observed at the other two temperatures. Figures 4(a) and 4(b) present the evolutions of the cluster number and the size of the largest cluster at 330 and 350 K, respectively. At 330 K, step I of the nucleation (H-O_{CB} fluctuation) terminates at about 3.6 ns, which is comparatively shorter than 7.5 ns at 350 K and 14.0 ns at 375 K. In step II, the rapid growth of the cluster is also accompanied with the sharp drop of the cluster number at 330 and 350 K,

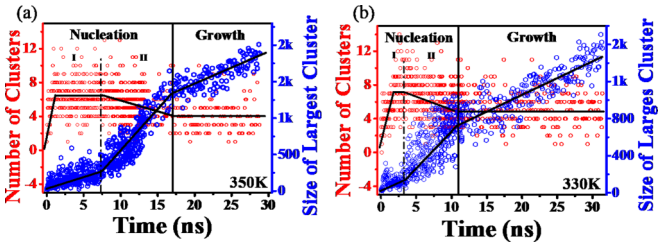

FIG. 4. The evolutions of the number of ordered clusters and the size of the largest cluster in a representative region of systems at 350 K (a) and 330 K (b), respectively.

confirming that the formation of stable orthorhombic nuclei follows the coalescence mechanism. Step II takes 7.7, 9.4, and 7.3 ns at 330, 350, and 375 K, which starts with sizes of the largest clusters of about 180, 250, and 300, while it ends with 800, 1350, and 1100, respectively. Lower temperature corresponds to a shorter time of step I and smaller cluster sizes at the onset of step II, while the time and the cluster size at the end of step II do not follow a monotonic trend with temperature, indicating that H-O_{CB} fluctuation in step I and the coupling between O_{CB} and density to form orthorhombic nuclei in step II have different temperature dependence.

III. DISCUSSIONS AND CONCLUSION

Based on the described analysis of the simulation results with two order parameters, including O_{CB} and density, crystal nucleation of PE is demonstrated to be assisted by the O_{CB} local structure order, which couples conformational and interchain rotational orders, in line with the two-step scenario observed in colloid systems. The precise kinetic pathway of PE crystal nucleation includes (I) H-O_{CB} fluctuation and (II) orthorhombic nucleation. Different from the stepwise growth process suggested by CNT [2], the formation of stable orthorhombic nuclei proceeds via the coalescence mechanism of neighboring H-O_{CB} clusters. Thereafter, crystal growth proceeds with increasing both lateral size and thickness. The movie [30] (see SM, movie 2) shows that crystal grains absorb neighboring H-O_{CB} clusters to achieve side expansion and simultaneous growth in chain direction through conformation adjustment, which looks rather similar to the multistage model proposed by Strobl [24], also found in other systems by De Yoreo *et al.* [32].

Intrachain conformational order is an intrinsic precondition of polymer crystallization which does not exist in simple spherical atoms. The Hoffman-Lauritzen [29] secondary nucleation model simply assumes that conformational ordered segments, with length the same as the lamellar thickness attached on the growth front, and the lateral surface free energy equals the entropic loss in conformational ordering of the segments [29]. Based on this hypothesis, the HL model takes conformational ordering as the rate-limiting factor in polymer crystallization. Olmsted *et al.* [25] proposed that coupling between conformational order and density induces liquid-liquid phase separation prior to crystallization. As density fluctuation is global in nature, both concentration and length of conformational ordered segments are required in these models. Focusing on the crystal growth front, the multistage crystallization model of Strobl [24] is composed of orientational order with long conformational ordered segments. Evidently, all these models take either concentration or length of conformational ordered segments as the precondition for preordering or nucleation, while the exact transformation from flexible chains into these conformational ordered segments with required length and concentration is not explicitly clarified yet. This challenge may be solved by O_{CB} local structure order as it is defined locally around particles. The results from performed simulations show that short *trans* segments are sufficient to arrange in H-O_{CB} ordered clusters without the required orientation (parallel packing) or density order. Without interchain coupling, thermal fluctuation may prevent *trans* segments of PE from growing in length and in concentration. Here we show that this issue is circumvented by the O_{CB} local structure order, which promotes the growths of *trans* segments and hexagonal clusters with low structure entropy S_2, even though they are still dynamic in nature. After the H-O_{CB} clusters reach a certain size, other orderings such as orientation and density may set in and eventually will result in crystal order. Another interesting observation is the coalescence of neighboring H-O_{CB} clusters in order to form stable orthorhombic nuclei. The existence of bond stretch, angle torsion, and conformation transition (*trans* to *gauche*) increase the free energy barrier for both forming and breaking a nuclei at the initial stage. In a polymer chain, the connectivity of monomers may indeed prefer to take a collective approach in nucleation and growth, like merging neighboring H-O_{CB} clusters.

The occurrence of O_{CB} fluctuation assisted nucleation in PE does not necessarily exclude the possibility of density fluctuation before crystal ordering, especially under nonequilibrium conditions like nonlinear flow [33–35]. Density fluctuation, as revealed by small-angle x-ray scattering, has been widely reported prior to the onset of crystal order. As suggested by theory and experiments for stretch-induced coil-helix transition [36,37], flow can also promote the transformation from a flexible chain to rigid conformational ordered segments, which may directly couple with density rather than local orders. Moreover, the existence of intrachain conformational order leads to a far more complex phase behavior than those in spherical atoms. Mutual coupling between two order parameters such as intrachain conformation order and interchain O_{CB} or density order may result in an isotropic-nematic transition or phase separation. These coupling mechanisms may explain the complex phase or self-assembly behaviors with various metastable structures in synthetic and biopolymers.

IV. METHODS

A. Simulation details

Full-atom MD simulations are performed with NAMD [38]; in order to reserve the conformation and stereo-hindrance effect of PE, the CHARMM force field is chosen with the parameters proposed by Yin and MacKerell *et al.* [39]. The system contains 32 PE chains with 500 monomers per chain, so there are about 100 000 atoms in the simulation box with a box size of 97, 113, and 84 Å in x, y, and z directions, respectively. The initial structure of amorphous PE is generated

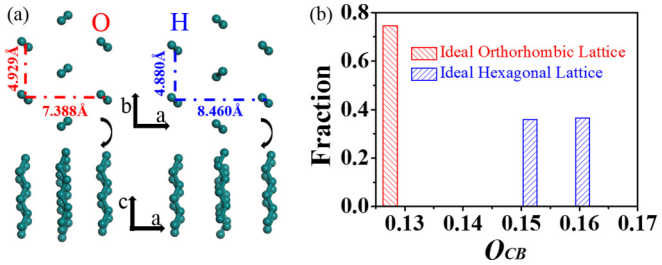

FIG. 5. (a) Ideal orthorhombic (left) and hexagonal (right) lattices of PE. (b) O_{CB} values of orthorhombic and hexagonal lattices. The orthorhombic structure has O_{CB} equal to 0.130, while O_{CB} for the hexagonal lattice equals 0.150 or 0.165, which are well separated from each other.

by random walk using MATERIALS STUDIO packages [40]. An *NPT* ensemble is set to control the whole system at pressure of 1 atm. After 2-ns relaxation at 600 K the initial structure of the PE melt was created with $\langle R^2\rangle/\langle R_g^2\rangle = 5.20 \pm 1.45$ (mean square end-to-end vector $\langle R^2\rangle$ over radius of gyration $\langle R_g^2\rangle$). The system is quenched to 330, 350, and 375 K to run dynamics over a time period of 28 ns, during which the time step is set as 1 fs. The periodic boundary conditions are imposed in three directions.

B. Parameter definition

The shape descriptor, the mathematical fingerprint to identify a local or global structure, has been widely used in diverse systems (colloidal, protein, and nanoparticles) [41]. The first step is to select a reference structure; herein the ideal orthorhombic and hexagonal lattices of PE at room temperature are built up as a reference in this work as shown in Fig. 5(a), left and right sides, respectively. The key step for a shape descriptor is to construct equations in order to convert the multidimensional structure into a mathematic index or similarity metric. Thereafter, the residuals between a query and reference structures can help achieve structure retrieval. Equations (2) and (3) are our converters, and Fig. 5(b) shows the "mathematic indices" (O_{CB}) for different referential structures. The O_{CB} value equals 0.130 and 0.150–0.165, corresponding to the center atom of orthorhombic cluster (*O-CA*) and hexagonal structure (*H-CA*), respectively. We calculate the number of O_{CB} structures in Figs. 1(d)–1(f) by counting the number of center atoms (CA). Q_l in Eq. (2) is a summation of several orders of spherical harmonic function Y_{lm}, where $l = 4$ and $m \in [0,l]$, θ_{ij} and φ_{ij} correspond to the polar and azimuthal angles, respectively. Equation (3) is the average operation, where $N_b(i)$ is the number of neighboring atoms j of center atom i within a cutoff distance of 5.4 Å. We also define O-O_{CB} and H-O_{CB} structures as center atoms together with their surrounding carbon atoms within a distance of 5.8 Å, which is larger than 5.4 Å in order to improve observation when reconstructing the ordered structures:

$$Q_l = \sum_{m=0}^{l} |Y_{lm}(\theta_{ij},\varphi_{ij})|^2, \tag{2}$$

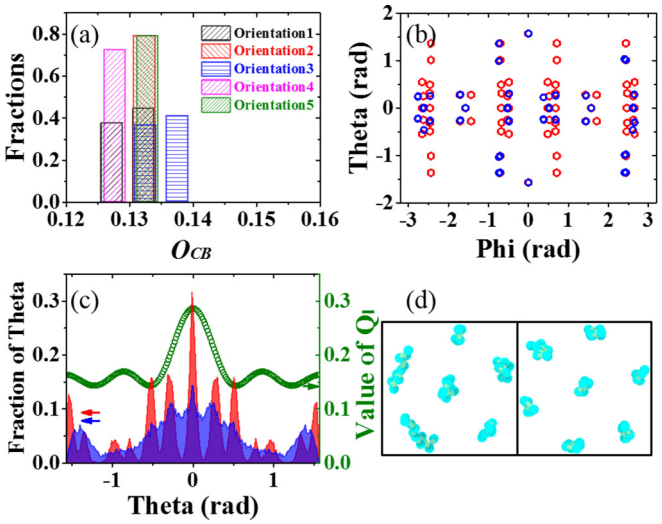

FIG. 6. (a) O_{CB} values of an ideal orthorhombic lattice with five random orientations, which indicate the "mathematic footprint" and do not change with orientation. (b) The distributions of φ and θ for orthorhombic and hexagonal lattices of PE, which indicate the connection between these two angles due to the *trans* conformation and parallel of neighboring segments. (c) The values of Q_l and θ distributions in the same domain $(-\pi/2, \pi/2)$, which indicates that the Q_l keeps most features of θ distributions. Red and blue dots correspond to orthorhombic and hexagonal structures in (b) and (c), respectively. (d) The structures we found by the O_{CB} parameter.

$$O_{CB} = \frac{1}{N_b(i)} \sum_{j=1}^{N_b(i)} \left(\frac{2\pi}{l+1} Q_l \right)^{1/2}. \tag{3}$$

C. The shape descriptor is constructed based on following considerations.

(a) Coordinate transform. One of the principal difficulties faced by our structure retrieval is the isotropy of the system, which means the orientation of the chain is unpredictable. The initial coordinate would lead to catastrophic consequences when adapting it into a "converter." Nevertheless, a certain center atom i and corresponding polar and azimuthal angles (θ_{ij} and φ_{ij}) with neighboring atoms j within 5.4 Å could be calculated as shown in Fig. 6(b). Even though the exact values of these angles would vary with orientation, the results of spherical harmonic function will be identical to rotational invariance. O_{CB} values of ideal orthorhombic lattices with five random orientations are shown in Fig. 6(a), while all O_{CB} values ≅0.13 demonstrate the rotational invariance. Therefore, we can exclude the effect of the orientation by transforming the coordinate from Descartes to a spherical and by choosing a proper spherical function as the "converter."

(b) Dimension reduction approximation. The relative spherical coordinate presents the distributions of θ_{ij} and φ_{ij}. Figure 6(b) shows the essential connections between these two angles for a reference structure that a given φ must correspond with several fixed θ due to the *trans* conformation. Matching query and ideal structures will be difficult, especially in the polymer system in the early stage of nucleation, if we

restrict both of them when constructing a "converter," as the connectivity and the flexibility of the chain create many kinds of defects. Herein, only considering the characteristic of θ_{ij} or φ_{ij} may be a better choice as the absolute value $|Y_{lm}(\theta_{ij},\varphi_{ij})|$ in Eq. (2) did, in terms of effectiveness and realism.

(c) Characteristic equations. Equations (2) and (3) were constructed to be the "converter" whose variables are φ and θ, which is convenient for the coordinate transformation. The absolute operation of Y_{lm} eliminates the effect of azimuthal angle φ. The features of θ distribution should be fully considered, as the information loss of φ and the proper range of m would help in constructing a converter. Figure 6(c) presents the contour of Q_l with summation of m from 0 to l (green dots) and the θ distributions of reference structures in the same domain $(-\pi/2, \pi/2)$. The characteristic peaks of ideal structures are well covered by Q_l, indicating the Q_l to be possibly a proper shape descriptor. Meanwhile, we assign conformational order as the precondition, because the PE crystals always ask for successive *trans* segments. *Trans* conformation also guarantees the mirror symmetry of θ distribution and can be regarded as a kind of compensation for discarding φ.

(d) Why average. The sum of squared residuals ($\Delta = \sum_{j=1}^{N_b(i)} |Q_l^{j\_\text{reference}} - Q_l^{j\_\text{query}}|^2$) should have been the best way to match a query and reference structure based on the value of Q_l if we had known the correspondence of every atom. Alternatively, we take the average over all the neighboring atoms, as was also done in Eq. (3), to create reference mathematic indices, see Fig. 5(b). This operation reduces accuracy remarkably, although it is sufficient for defining local structural order in PE systems, which may be partially due to the fact that conformational order is taken as the precondition. A prediction could be made based on the above discussions, ensuring that a slight tilt of neighboring chains will not change the O_{CB} value significantly, as the θ distribution only goes through a small shifts. As shown by the simulation results [Fig. 6(c), SM movie 1], local order structures of extracted (H-O_{CB}) can be organized by *trans* segments tilted with each other.

ACKNOWLEDGMENTS

The authors would like to thank Prof. Daan Frenkel (Cambridge), Prof. Stephen Cheng (Akron), Prof. Ning Xu (USTC), and Prof. Haojun Liang (USTC) for fruitful discussion on simulation and data interpretation. The National Supercomputing Center in Shenzhen, Supercomputing Center of University of Science and Technology of China, and National Supercomputer Center in Tianjin [TianHe-1(A)] are acknowledged for providing the computational resources. This work is financially supported by National Natural Science Foundation of China (Contracts No. 51633009 and No. 51325301) and also in part supported by the China Postdoctoral Science Foundation (Grant No. 2016M602015).

[1] S. Z. D. Cheng, *Phase Transitions in Polymers, The Role of Metastable States* (Elsevier Ltd., New York, 2008).
[2] D. Turnbull and J. C. Fisher, J. Chem. Phys. **17**, 71 (1949).
[3] J. D. Mccoy, K. G. Honnell, K. S. Schweizer, and J. G. Curro, J. Chem. Phys. **95**, 9348 (1991).
[4] S. Auer and D. Frenkel, Nature (London) **409**, 1020 (2001).
[5] P. R. ten Wolde and D. Frenkel, Science **277**, 1975 (1997).
[6] T. Kawasaki and H. Tanaka, Proc. Natl. Acad. Sci. USA **107**, 14036 (2010).
[7] A. Haji-Akbari and P. G. Debenedetti, Proc. Natl. Acad. Sci. USA **112**, 10582 (2015).
[8] J. Zierenberg, P. Schierz, and W. Janke, Nat. Commun. **8**, 14546 (2017).
[9] P. Rein ten Wolde, M. J. Ruiz-Montero, and D. Frenkel, J. Chem. Phys. **104**, 9932 (1996).
[10] J. C. Palmer, F. Martelli, Y. Liu, R. Car, A. Z. Panagiotopoulos, and P. G. Debenedetti, Nature (London) **510**, 385 (2014).
[11] M. Salvalaglio, C. Perego, F. Giberti, M. Mazzotti, and M. Parrinello, Proc. Natl. Acad. Sci. USA **112**, E6 (2015).
[12] P. Tan, N. Xu, and L. Xu, Nat. Phys. **10**, 73 (2013).
[13] Y. L. Wu, D. Derks, A. van Blaaderen, and A. Imhof, Proc. Natl. Acad. Sci. USA **106**, 10564 (2009).
[14] H. J. Schope, G. Bryant, and W. van Megen, Phys. Rev. Lett. **96**, 175701 (2006).
[15] W. Qi, Y. Peng, Y. Han, R. K. Bowles, and M. Dijkstra, Phys. Rev. Lett. **115**, 185701 (2015).
[16] D. M. Herlach, T. Palberg, I. Klassen, S. Klein, and R. Kobold, J. Chem. Phys. **145**, 211703 (2016).
[17] M. Sleutel and A. E. S. Van Driessche, Proc. Natl. Acad. Sci. USA **111**, E546 (2014).
[18] P. Welch and M. Muthukumar, Phys. Rev. Lett. **87**, 218302 (2001).
[19] M. Anwar, J. T. Berryman, and T. Schilling, J. Chem. Phys. **141**, 124910 (2014).
[20] C. Hyeon, G. Morrison, D. L. Pincus, and D. Thirumalai, Proc. Natl. Acad. Sci. USA **106**, 20288 (2009).
[21] T. Yamazaki, Y. Kimura, P. G. Vekilov, E. Furukawa, M. Shirai, H. Matsumoto, A. E. S. Van Driessche, and K. Tsukamoto, Proc. Natl. Acad. Sci. USA **114**, 2154 (2017).
[22] J. Yang, X. Tang, Z. Wang, T. Xu, F. Tian, Y. Ji, and L. Li, J. Chem. Phys. **146**, 014901 (2017).
[23] M. L. Wallace and B. Joós, Phys. Rev. Lett. **96**, 025501 (2006).
[24] G. Strobl, Rev. Mod. Phys. **81**, 1287 (2009).
[25] P. D. Olmsted, W. C. K. Poon, T. C. B. McLeish, N. J. Terrill, and A. J. Ryan, Phys. Rev. Lett. **81**, 373 (1998).
[26] J. Xu, Y. Ma, W. Hu, M. Rehahn, and G. Reiter, Nat. Mater. **8**, 348 (2009).
[27] C. Luo and J. U. Sommer, Phys. Rev. Lett. **112**, 195702 (2014).
[28] T. Yamamoto, Macromolecules **43**, 9384 (2010).
[29] J. D. Hoffman and R. L. Miller, Polymer (Guildf.) **38**, 3151 (1997).
[30] See Supplemental Material at http://link.aps.org/supplemental/10.1103/PhysRevMaterials.1.073401 for two movies are provided to show the OCB structures we found and the coalescing process of neighboring H-OCB structures. Other information including conformational order, comparison of Voronoi volume between melt and H-OCBs and some adjacent-averaged data are also presented.
[31] T. M. Truskett, S. Torquato, and P. G. Debenedetti, Phys. Rev. E **62**, 993 (2000).

[32] J. J. De Yoreo, S. Whitelam, D. Joester, H. Zhang, J. D. Rimer, A. Navrotsky, J. F. Banfield, A. F. Wallace, F. M. Michel, F. C. Meldrum, H. Cölfen, and P. M. Dove, Science **349**, aaa6760 (2015).
[33] B. S. Hsiao, L. Yang, R. H. Somani, C. A. Avila-Orta, and L. Zhu, Phys. Rev. Lett. **94**, 117802 (2005).
[34] Z. Wang, J. Ju, J. Yang, Z. Ma, D. Liu, K. Cui, H. Yang, J. Chang, N. Huang, and L. Li, Sci. Rep. **6**, 32968 (2016).
[35] R. S. Graham and P. D. Olmsted, Phys. Rev. Lett. **103**, 115702 (2009).
[36] S. Courty, J. L. Gornall, and E. M. Terentjev, Proc. Natl. Acad. Sci. USA **102**, 13457 (2005).
[37] A. Buhot and A. Halperin, Phys. Rev. Lett. **84**, 2160 (2000).
[38] J. C. Phillips, R. Braun, W. Wang, J. Gumbart, E. Tajkhorshid, E. Villa, C. Chipot, R. D. Skeel, L. Kale, and K. Schulten, J. Comput. Chem. **26**, 1781 (2005).
[39] D. Yin and A. D. MacKerell, J. Comput. Chem. **19**, 334 (1998).
[40] Accelrys Software, Accelrys Software, Inc., San Diego, CA, 2012.
[41] A. S. Keys, C. R. Iacovella, and S. C. Glotzer, Annu. Rev. Condens. Matter Phys. **2**, 263 (2011).